Transition from internal to external oxidation in indium–silver alloys[1]

L. D. PETHE, H. B. MATHUR,[2] AND A. B. BISWAS[3]

National Chemical Laboratory, Poona, India

The kinetics of oxidation of In–Ag alloys of 5, 10, and 15 at. % indium have been studied on a vacuum microbalance. The 15 at. % indium alloy oxidizes externally and the 5 at. % alloy internally. A plot of logarithm of the parabolic oxidation rate, k_p, versus reciprocal of the absolute temperature for 10 at. % indium alloy gives two intersecting straight lines corresponding to the energies of activation of 23 and 39.6 kcal/mole for the oxidation below and above 600 °C respectively. These are comparable to the energies of activation of 23 kcal/mole for the internal oxidation of 5 at. % indium alloy and 40 kcal/mole for the external oxidation of 15 at. % indium alloy. The rate-controlling step in the external oxidation of 15 at. % indium alloy is the diffusion of indium through the alloy. Photomicrographs of the cross sections of the oxidized foils of these alloys confirm the conclusions derived from the kinetic data.

The high temperature oxidation studies on a series of alloys by Rhines *et al.* (1–3) and Meijering and Druyvesteyn (4) have provided the basis on which the general features of internal oxidation can be adequately explained. When the percentage of the baser metal component in a binary alloy is increased to a certain critical value, the volume of the precipitated oxide of the baser metal becomes so large that its particles condense to form a barrier which inhibits further oxygen diffusion through the alloy matrix, resulting in the transition from internal to external oxidation. Dietrich and Koch (5) found this critical concentration to be 9 atom % indium for In–Ag alloy. Wagner (6) has described the conditions required for this transition mathematically in terms of the diffusion rates of oxygen and the oxide forming baser metal and the molar volumes of the metal and the oxide. Rapp (7) evaluated this theory for the In–Ag system and found his experimental results at 550 °C in agreement with Wagner's theoretical predictions. More recently he has also studied the oxidation of three In–Ag alloys of less than 15 atom % indium, based on the computer-calculated programs for the formation of interruption bands (8). The change in the mechanism of oxidation of indium–silver alloys appears to be solely dependent on the concentration of the less noble metal. However, the kinetics of oxidation have not been studied

systematically over a range of temperature in the region of the critical concentration. In this communication, we report the results of such an investigation with the aid of a quartz microbalance.

Experimental Procedure

The quartz microbalance was constructed according to the details described by Bradley (9). As the density of the In–Ag alloy was nearly the same as that of pure silver, the counterpoise weights were prepared from pure silver in order to eliminate corrections due to buoyancy. The sample was suspended in the constant temperature zone of nearly 3.0 cm in the middle of a non-inductively wound resistance furnace.

After suspending the sample the reaction vessel was evacuated to 10^{-5} Torr. Argon was then introduced at the experimental pressure. The furnace, controlled and set at the experimental temperature, was raised over the reaction vessel. The sample was annealed at the experimental temperature for 1 h. Argon was then pumped out and oxygen introduced in its place. The rate of oxidation was then followed by noting the movement of the reference pointer, fixed to the balance beam. As the molecular weights of argon and oxygen are nearly equal, the above procedure enabled us to determine the position of the moving pointer before oxidation started and at the same time avoided corrections due to buoyancy and the thermomolecular effects.

Silver–indium alloys were prepared by melting the spectroscopically pure metals in high purity graphite crucibles, placed inside silica tubes and sealed in a vacuum of 10^{-5} Torr. The metals had the following analysis.

Silver Fe, 0.03 %; Si, 0.01 %; Mg, 0.003 %; Al, 0.003 %; and Cu, 0.003 %.

Indium Fe, Pb, Sn, Mg, Ag, each 0.003 %; Bi and Ni each 0.001 %; Si, 0.0003 %.

The homogenity of the alloys was tested by the analysis of small fractions of the alloy taken from different portions of the ingot. The ingots were cold rolled to foils of the desired thickness. The foils were abraded successively by 2/0 and 4/0 emery papers under mineral oil, rinsed in low boiling point petroleum ether, and finally suspended in the balance.
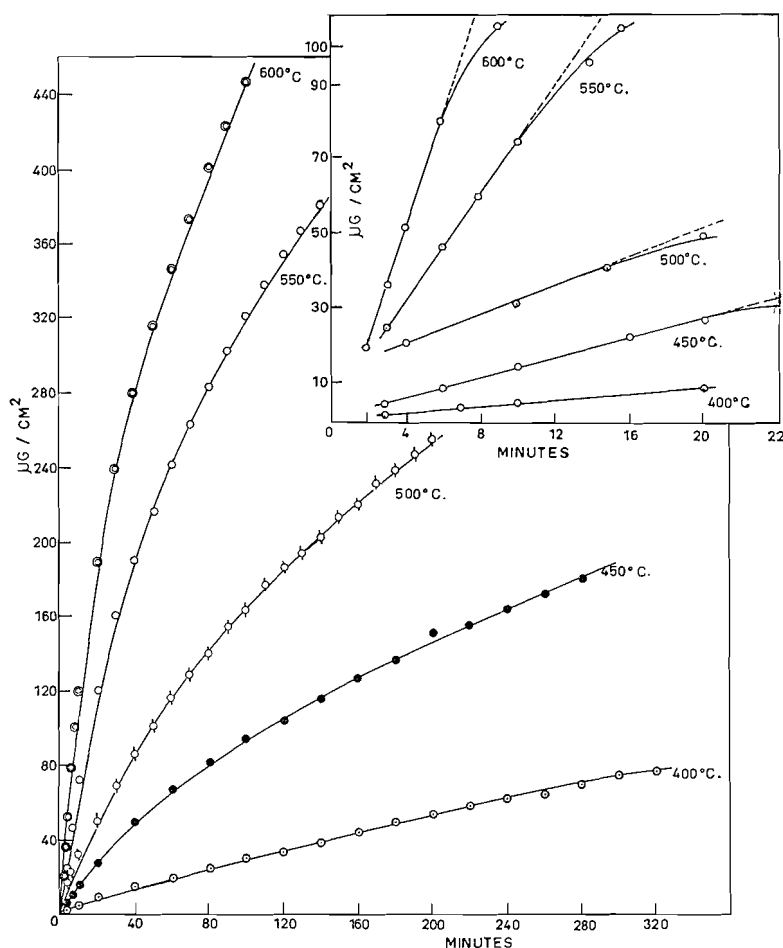
FIG. 1.   Kinetics of oxidation of 5/95 In–Ag alloy in 76 Torr oxygen pressure at various temperatures. The initial rate of oxidation of the alloy is shown in the enlarged figure at the top right hand corner.

Spectroscopically pure argon was used and oxygen gas was prepared from analytical reagent grade potassium permanganate.

Results and Discussion

The oxidation studies were undertaken on three alloys of silver containing 5, 10, and 15 atom % indium. The kinetics of oxidation of 5/95 In–Ag alloy in the region 400–600 °C and at 76 Torr oxygen pressure are represented in Fig. 1. The experimental data for all the three alloys have been plotted in Figs. 2–4 as the square of the oxygen uptake versus time.

It may be observed that the rate of oxygen uptake by the alloys decreases sharply with the increase in the indium content. With the excep-

tion of a brief initial period, the oxidation of 5 at. % In–Ag alloy in the temperature interval 450–600 °C can be described by means of a parabolic rate law. The rate of oxidation for the first few minutes shows a linear dependence with time as shown in Fig. 1. The interval during which the linear law is obeyed increases with the decrease in temperature. At 400 °C, the oxidation during the entire period of study can be described by a linear rate law. The oxidation kinetics of the 10 at. % In–Ag alloy are also governed by the parabolic rate law, the only exception being the experiment at 675 °C, where the oxidation kinetics deviates from the parabolic rate law after the 80th minute (Fig. 3). For the 15 at. % In–Ag alloy, the parabolic rate law is valid for
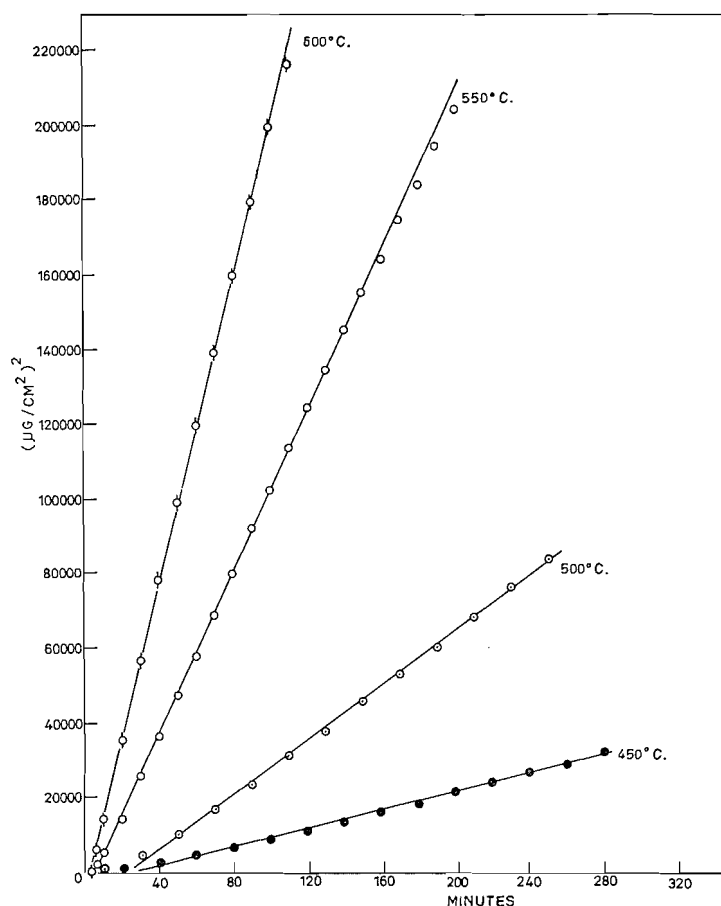
FIG. 2.   Parabolic plot of the oxidation of 5/95 In–Ag alloy.

an initial period. With an increase in the period of oxidation, marked departures from the parabolic rate law are observed. The period, over which the parabolic rate law is valid, decreases with an increase in the temperature of oxidation (Fig. 4).

The Arrhenius plots of the parabolic rate constants (Fig. 5) indicate that a single mechanism is responsible for the oxidation of 5 and 15 at. % In–Ag alloys while there are two different processes taking part during the oxidation of 10/90 In–Ag alloy. The change in the mechanism of oxidation takes place at about 600 °C. The obedience of the oxidation kinetics of the 5, 10, 15 at. % In–Ag alloys to the parabolic rate law indicates that the diffusion is the rate-controlling process during their oxidation. The initial linear rate, observed in 5/95 In–Ag alloy,

is due to a phase boundary reaction where the dissociation and dissolution of oxygen takes place at the alloy/oxygen interface. Indium atoms act as active sites for the dissociation of the oxygen before it dissolves in the alloy. This gives rise to and maintains the concentration gradient within the alloy which acts as the driving force for the diffusion of oxygen. Once the concentration gradient has been built up, further oxidation is controlled by the diffusion of oxygen through the alloy. The observed linear rate of oxidation at 400 °C indicates that the phase boundary reaction is the rate-controlling step during the entire period of oxidation.

The energies of activation calculated for the oxidation of these alloys from the Arrhenius plots in Fig. 5 are summarized in Table I.
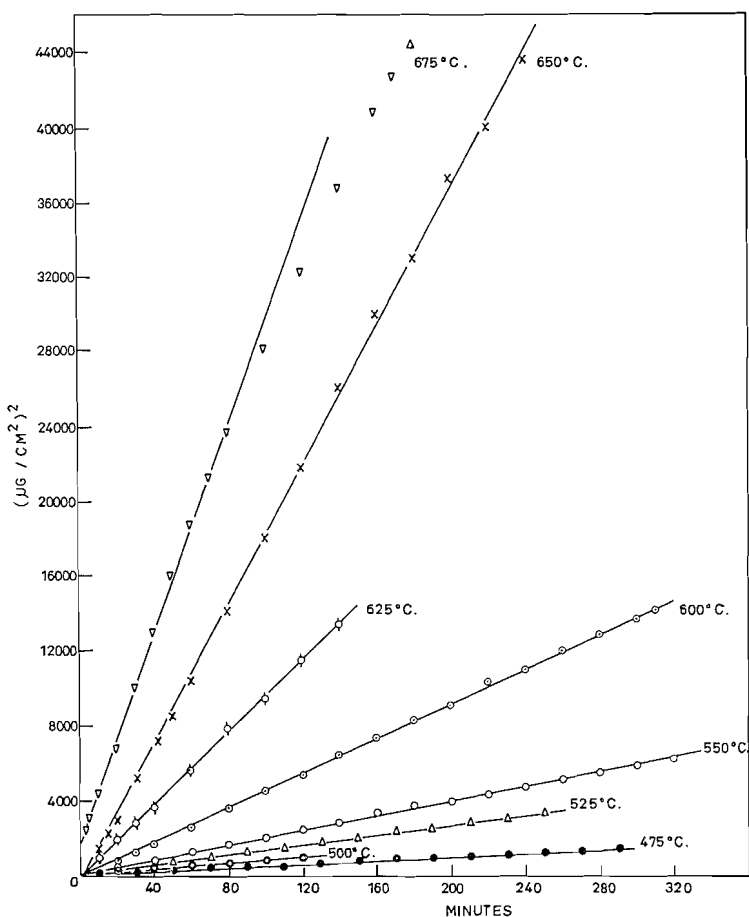
The energy of activation of 23.6 kcal/$\frac{1}{2}$mole

FIG. 3. Parabolic plot of the oxidation of 10/90 In–Ag alloy.

TABLE I

The energies of activation calculated from the slopes of the Arrhenius plots in Fig. 5 for the oxidation of 5, 10, and 15 atom % In–Ag alloys

In–Ag alloy (atom % In)	Activation energy (kcal/mole)
5	23.6
10	23.0, 39.6
15	40.0

observed in the oxidation of 5/95 In–Ag alloy corresponds to internal oxidation. According to Rapp's (7) equation [14], the parabolic constant for internal oxidation is proportional to the product of the oxygen solubility $N_O^{(s)}$ and oxygen diffusivity D_O. Hence,

$$\frac{d[\ln K_p]}{dT} = \frac{d[\ln N_O^{(s)}]}{dT} + \frac{d[\ln D_O]}{dT} =$$

$$\frac{1}{RT^2}[\Delta H\{\tfrac{1}{2}O_2(g) =$$

$$O_{(in\ Ag)}\}] + \frac{\Delta E_{(diff)}}{RT^2}.$$

According to Eichenauer and Muller (10)

$$\Delta H[\tfrac{1}{2}O_2(g) = O_{(in\ Ag)}] = 11.86\ kcal.$$
$$\Delta E_{(diff)} = 11.00\ kcal.$$

Hence,

$$\frac{d\ln K_p}{dT} = \frac{11.86 + 11.00}{RT^2} = \frac{22.86}{RT^2}.$$

The calculated activation energy of 22.86 kcal/$\tfrac{1}{2}$mole O_2 for the parabolic kinetics is in
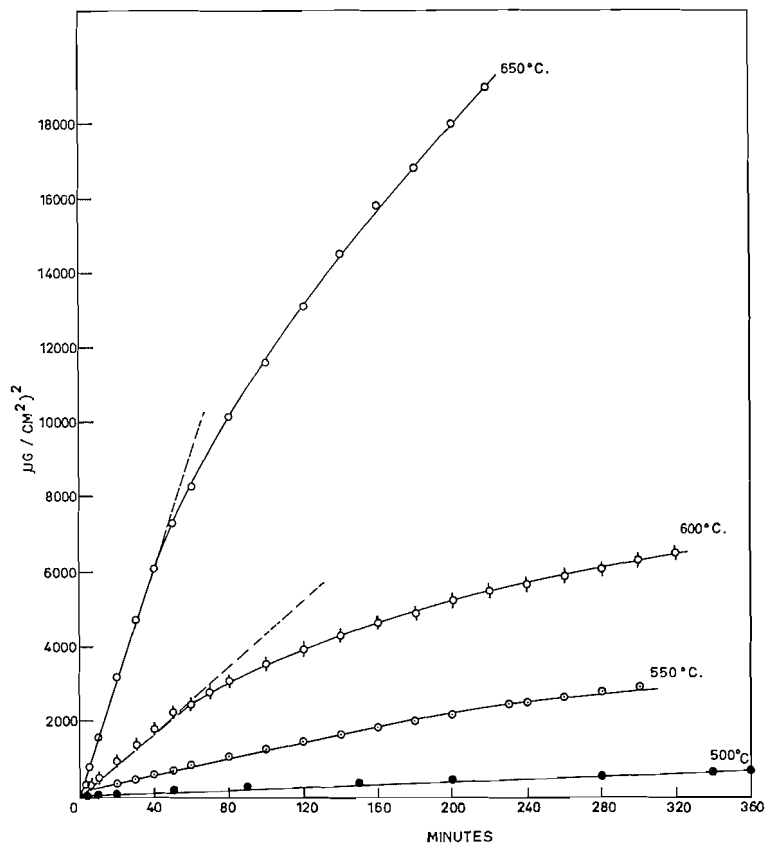
FIG. 4.   Parabolic plot of the oxidation of 15/85 In–Ag alloy.

good agreement with the value of 23.6 kcal/mole deduced from the experimental temperature dependence of K_p.

The rate of oxidation of the 15/85 In–Ag alloy has been found to be much lower than that of the 5/95 In–Ag alloy. This is due to the formation of an external oxide layer. The growth of this external scale is controlled by the diffusion of indium ions through it. The oxide was identified as In_2O_3 by electron diffraction.

The energy of activation for the 15/85 In–Ag alloy has been found to be 40.05 kcal/mole and is comparable to the energy of activation of 36.6 kcal/mole reported by Schoen (11) for the diffusion of In through 16.6/93.4 In–Ag alloy. This suggests that the rate-controlling step during the oxidation of 15/85 In–Ag alloy is the diffusion of In through the alloy and not through the oxide as assumed by Rapp (7). An interrupted oxidation of 15/85 In–Ag alloy at 600 °C (described below) supports the above conclusion.

The parabolic law ceases to hold after a certain period of oxidation of the 15/85 In–Ag alloy (Fig. 4). Such a deviation can either be (1) due to the ageing of the oxide layer (12) or (2) due to a decreased diffusion of indium through the oxide on account of the depletion of indium atoms at the alloy/oxide interface. In order to find out which of the two mechanisms is responsible for the deviation, the following experiment was carried out.

A sample of 15/85 In–Ag alloy foil was oxidized at 600 °C and at 76 Torr oxygen pressure for 40 min (the period estimated from the data in Fig. 4), after which the deviation from the parabolic rate law is expected to take place. The oxygen was then replaced by argon at the same pressure. The sample was annealed at the same temperature for 60 min, after which argon was replaced by oxygen and the oxidation reaction continued. The kinetic and the parabolic plots for this experiment (Fig. 6) show that the
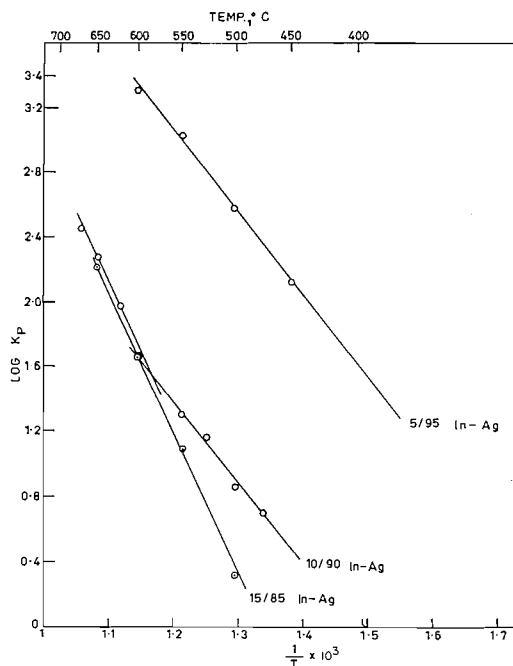
FIG. 5. The variation of logarithm of the parabolic rates of oxidation of 5, 10, and 15 at. % In–Ag alloys as a function of reciprocal of absolute temperature.

interrupted oxidation can still be described by a parabolic rate law in spite of the fact that in a normal conventional run, a deviation from this rate law takes place. This deviation is due to the depletion of the indium atoms at the alloy/oxide interface. In_2O_3 is a n-type semiconductor (13) and the growth of In_2O_3 oxide layer may be assumed to take place through the diffusion of interstitial In^{3+} ions through the oxide matrix. If the rate at which the indium atoms are delivered at the alloy/oxide interface is lower than the diffusion rate of indium ions through the oxide, the former step would be rate controlling. If, however, the oxidized sample is annealed in an inert atmosphere, as is done in our interrupted oxidation experiment, the concentration of In in the alloy layer immediately below the alloy/oxide interface would be restored to nearly its original value as a result of the inward diffusion of Ag atoms and the outward diffusion of In atoms during the annealing. This would restore the oxidation kinetics to the parabolic rate law. The oxygen uptake for the first 10 min immediately after the inert gas annealing is higher than the oxygen uptake for the same period immediately

preceding the interruption of oxidation as shown in Fig. 6. This observation would immediately rule out the ageing of the oxide film as the cause of the reduction in the oxidation rate of the 15/85 In–Ag alloy at 600 °C (Fig. 4) because ageing of the oxide film would have resulted in a lowering of the oxidation rate. If the oxidation data obtained after the inert gas annealing are plotted according to a parabolic equation by assuming the 100th minute as the zero of the time scale, a parabolic rate constant $k_p = 45$ $\mu g^2/cm^4$ min is obtained. This may be compared with the value of $k_p = 43.5$ $\mu g^2/cm^4$ min during oxidation prior to annealing. Almost equal values of the parabolic rate constants support the conclusions derived earlier.

The energy of activation for the oxidation of 10/90 In–Ag alloy below 600 °C is 23.0 kcal/$\frac{1}{2}$mole and is comparable to the energy of activation of 23.6 kcal/$\frac{1}{2}$mole for the internal oxidation of 5/95 In–Ag alloy (Table I). On the other hand, the energy of activation of 39.6 kcal/mole for the oxidation of this alloy above 600 °C can be attributed to the external oxidation, since it is nearly equal to 40.0 kcal/mole, the activation energy for the external oxidation of 15/85 In–Ag alloy. Hence we conclude that the 10/90 In–Ag alloy oxidizes predominantly internally below 600 °C while it undergoes predominantly external oxidation above 600 °C. In fact, a reduction in the rate of oxidation of 15/85 In–Ag alloy with an increase in the period of oxidation observed at all temperatures (Fig. 4) has also been found in the oxidation rate of 10/90 In–Ag at 675 °C (Fig. 3). This is expected at higher temperatures since the oxide molecules have a higher mobility which facilitates the formation of coarser oxide particles. They obstruct further diffusion of oxygen and hence inhibit internal oxidation. At lower temperatures the oxide molecules are relatively immobile and are dispersed widely as small oxide particles which may not form a barrier to the diffusion of oxygen. This is the cause of the transition from the internal oxidation to the external oxidation of the 10/90 In–Ag alloy at 600 °C. It may be expected that such a transition can also take place in alloys of lower indium contents like the 5/95 In–Ag but only at comparatively higher temperatures.

Photomicrographs of the cross sections of the foils of the three alloys oxidized at 600 °C and 76 Torr oxygen pressure support the above
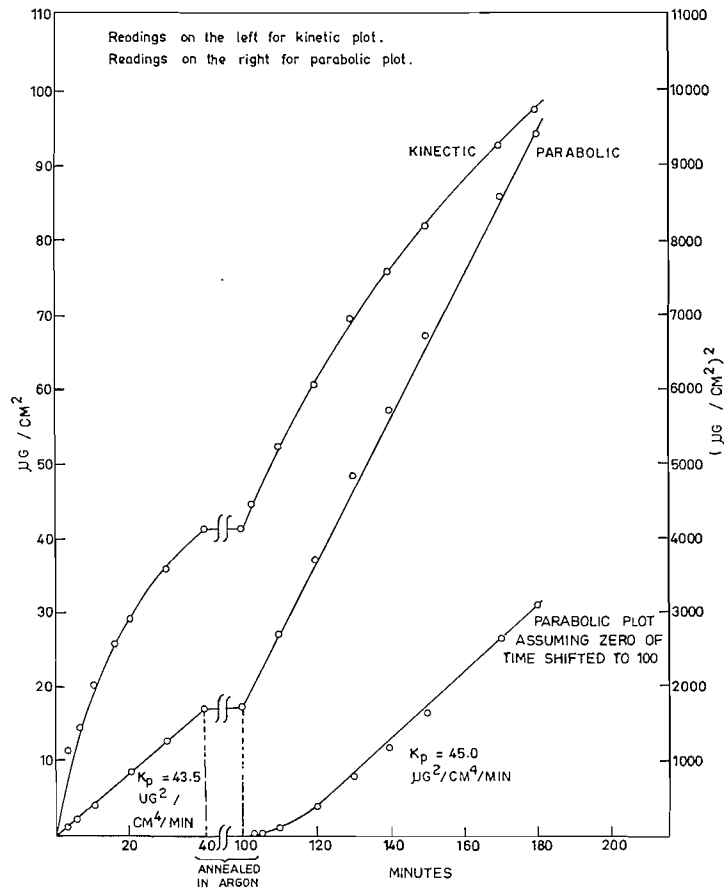
FIG. 6.   Oxidation of 15/85 In–Ag alloy at 600 °C and 76 Torr oxygen pressure. The oxidation was interrupted between the 40th and 100th minute by pumping out oxygen from the reaction vessel.

conclusions. Figure 7 shows the two oxidation fronts advancing parallel to the surface of the internally oxidized foil of 5/95 In–Ag alloy. The precipitation of the oxide at the grain boundaries is clearly indicated. Figure 8 shows the cross section of the oxidized 10/90 In–Ag alloy. This alloy oxidizes both internally and externally. Hence, we observe significant precipitation at the grain boundaries, as well as the external oxide scale. The latter is not visible in the photograph due to the uneven rates of dissolution of the alloy and oxide during etching. In contrast to this, Fig. 7 shows no unevenness of the external layer since no external oxide is present. A cross section of the 15/85 In–Ag oxidized foil shown in Fig. 9 indicates that there is no significant precipitation at the grain boundaries and only an external scale is formed, as is evident from the unevenness of the surface.

The process of internal oxidation can be considered to take place in the following three consecutive steps: (a) dissociation of oxygen molecules to atoms at the phase boundary, (b) dissolution of oxygen atoms in the alloy, and (c) diffusion of oxygen atoms in the alloy away from the surface.

If the interface reactions (a) and (b) are the rate-controlling steps, it is expected that the oxidation would be governed by a linear rate (14). On the other hand, if step (c) is rate controlling, we expect the oxidation to be governed by the parabolic rate law. It may be noted that the initial linearity of the oxidation rate for 5/95 In–Ag alloy may be due to the steps (a) or (b), or both controlling the rate of oxidation. A plot of the logarithm of the linear rate constant versus $1/T$ is a straight line (Fig. 10) and the energy of activation calculated from its slope is

FIG. 7.   The cross section of the 5/95 In–Ag alloy foil after oxidation at 600 °C in 76 Torr oxygen pressure for 2 h. The lighter band in the middle is the unoxidized alloy.

FIG. 8.   The cross section of the 10/90 In–Ag alloy after oxidation at 600 °C in 76 Torr oxygen pressure for 4 h.

FIG. 9.   The cross section of 15/85 In–Ag alloy foil after oxidation in 76 Torr oxygen pressure at 600 °C for 4 h. The unevenness of the surface is due to the external oxide layer.
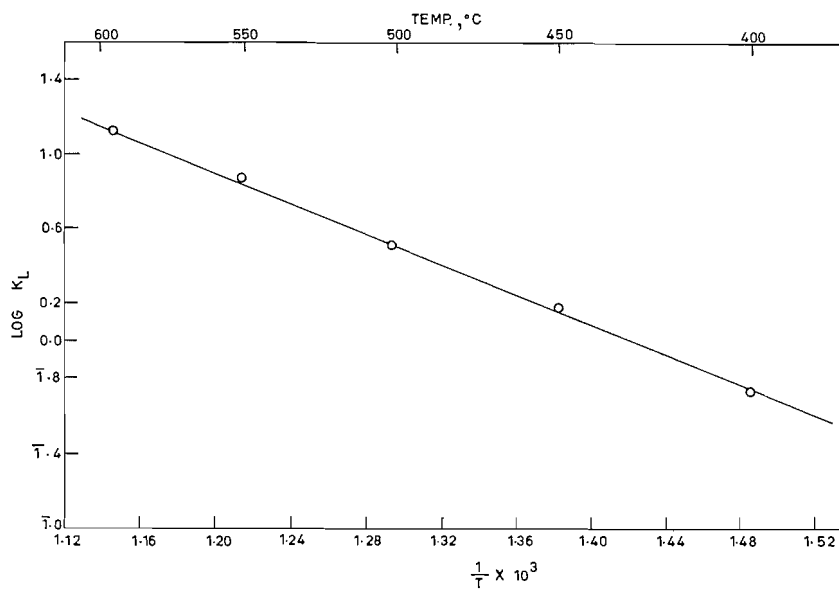

FIG. 10.   Variation of the logarithm of linear rate of oxidation of 5/95 In–Ag alloy as a function of the reciprocal of absolute temperature.

18.5 kcal/$\frac{1}{2}$mole O_2. This is very much lower than the energy of activation required for the dissociation of oxygen, viz. 59 kcal/$\frac{1}{2}$mole (15), but is of the same order of magnitude as the energy of activation of 11.86 kcal/$\frac{1}{2}$mole O_2 found for dissolution of oxygen in pure silver (10). It is therefore suggested that the step (b), viz. the dissolution of oxygen atoms at the phase boundary, is the rate-controlling step and responsible for the initial linear oxidation rate of the 5/95 In–Ag alloy. It may, however, be noted that the observed energy of activation of 18.5 kcal/$\frac{1}{2}$mole O_2 is for the dissolution of oxygen in the 5/95 In–Ag alloy and hence is likely to be higher than that for pure silver.

1. F. N. RHINES and A. H. GROBE. Trans. Am. Inst. Mining Met. Engrs. 147, 318 (1942).
2. F. N. RHINES. Trans. Am. Inst. Mining Met. Engrs. 137, 246 (1940).
3. F. N. RHINES, W. A. JOHNSON, and W. A. ANDERSON. Trans. Am. Inst. Mining Met. Engrs. 147, 205 (1942).
4. J. L. MEIJERING and M. J. DRUYVESTEYN. Philips Res. Rept. 2, 81 (1947).
5. I. DIETRICH and L. KOCH. Z. Metallk. 50, 31 (1959).
6. C. WAGNER. Z. Elektrochem. 63, 772 (1961).
7. R. A. RAPP. Acta Met. 9, 730 (1961).
8. R. A. RAPP, D. F. FRANK, and J. V. ARMITAGE. Acta Met. 12, 508 (1963).
9. R. S. BRADLEY. J. Sci. Instr. 30, 84 (1953).
10. W. EICHENAUER and G. MULLER. Z. Metallk. 53, 321 and 700 (1962).
11. A. SCHOEN. Ph.D. Thesis, Physics Department, University of Illinois. 1958.
12. J. L. MEIJERING and M. L. VERHEIJKE. Acta Met. 7, 331 (1959).
13. O. KUBASCHEWSKI and B. E. HOPKINS. Oxidation of metals and alloys. Butterworth Publications, London. 1962. p. 24.
14. O. KUBASCHEWSKI and B. E. HOPKINS. Oxidation of metals and alloys. Butterworth Publications, London. 1962. p. 110.
15. T. L. COTTRELL. The strength of chemical bonds. Butterworth Scientific Publications, London. 1954.